The Effect of DNA Structure on the Catalytic Efficiency and Fidelity of Human DNA Polymerase β on Templates with Platinum-DNA Adducts*

Alexandra Vaisman‡, Matthew W. Warren, and Stephen G. Chaney§

From the Department of Biochemistry and Biophysics, Lineberger Comprehensive Cancer Center, School of Medicine, University of North Carolina, Chapel Hill, North Carolina 27599-7260

DNA adducts formed by platinum-based anticancer drugs interfere with DNA replication. The carrier ligand of the platinum compound is likely to affect the conformation of the Pt-DNA adducts. In addition, the conformation of the adduct can also change upon binding of damaged DNA to the active site of DNA polymerase. From the crystal structures of pol β ternary complexes it is evident that undamaged gapped and primed single-stranded (non-gapped) DNA templates exist in very different conformations when bound to pol β. Therefore, one might expect that the constraints imposed on the damaged templates by binding to the polymerase active site should also affect the conformation of the Pt-DNA adducts and their ability to inhibit DNA replication. In support of this hypothesis we have found that the efficiency, carrier ligand specificity, site of discrimination (3′-G *versus* 5′-G of the Pt-GG adducts), and fidelity of translesion synthesis past Pt-DNA adducts by pol β are strongly affected by the structure of the DNA template. Previous studies have suggested that the conformation of Pt-DNA adducts may be affected by the sequence context of the adduct. In support of this hypothesis, our data show that sequence context affects the efficiency, fidelity, and pattern of misincorporation by pol β.

Platinum-based chemotherapeutic drugs exert their cytotoxic effect through binding to DNA. *cis*-diaminedichloroplatinum(II)(cisplatin)[1] (Fig. 1), which has been broadly used for cancer treatment since 1978, and (*trans-R,R*)-1,2-diaminocyclohexaneoxalatoplatinum(II) (oxaliplatin) (Fig. 1), which is currently in clinical trial in the United States and has been approved in several European countries for the treatment of tumors with intrinsic and acquired resistance to cisplatin, both form the same types adducts on the DNA (1, 2). Although the most prevalent lesions created by interaction of both these agents with DNA are bifunctional intrastrand 1,2-d(GpG)

cross-links, these adducts differ in the carrier ligands they retain upon binding to DNA. Pt-DNA adducts formed by oxaliplatin contain (*trans-R,R*)-1,2-diaminocyclohexane (dach) carrier ligands, whereas the adducts formed by cisplatin contain *cis*-diammine carrier ligands. Structures of the DNA containing cisplatin-GG adducts determined by NMR and x-ray crystallography reveal significant distortion of base pairs in the vicinity of the adduct (3–6). In addition, both the crystallographic and NMR structures show that the cisplatin adduct causes a large positive roll in the helix resulting in compression of the major groove and widening of the minor groove. Although the conformation of oxaliplatin-GG adducts has not yet been determined experimentally, a recent molecular modeling study suggests that the overall conformation of cisplatin- and oxaliplatin-GG adducts are likely to be very similar. However, the bulky dach ring of the oxaliplatin adduct fills much of the DNA major groove, causing it to be narrower and less polar in the area of the adduct. These subtle differences in overall DNA conformation appear to influence the biological effects of the Pt-DNA adducts. Thus, both the mismatch repair complex (7) and high mobility group proteins (8) bind more strongly to cisplatin-GG adducts than to oxaliplatin-GG adducts. In addition, eukaryotic DNA polymerases β, γ, ζ, and η bypass oxaliplatin-GG adducts more readily than cisplatin-GG adducts (8–10). Finally, the misincorporation frequency of DNA polymerase β (pol β) is slightly greater with oxaliplatin-GG adducts than with cisplatin-GG adducts on primed single-stranded DNA (9). These data suggest that differences in the conformation of oxaliplatin- and cisplatin-GG adducts can affect both the efficiency and fidelity of translesion synthesis by DNA polymerases, which could at least partially account for differences in the cytotoxicity and mutagenicity of these Pt-DNA adducts.

The conformation of Pt-DNA adducts in the active site of DNA polymerases is likely to be different from that of adducted DNA in solution. The fact that DNA templates are often bent upon binding to the active site of DNA polymerases (11) supports this hypothesis. Unfortunately, whereas the conformation of mutagenic DNA adducts has been determined on a variety of duplex DNAs in solution, relatively little is known about how binding of the DNA templates to a polymerase active site affects the conformation of the adduct and/or the nascent base pair. The conformation of Pt-DNA adducts is clearly not identical in all DNA polymerase active sites. Whereas pol β, γ, ζ, and η all bypass oxaliplatin adducts better than cisplatin adducts, HIV-1 reverse transcriptase does not discriminate between cisplatin and oxaliplatin adducts (8–10). In addition, pol β, γ, ζ, and η differ in the site of replication termination, the site of discrimination between cisplatin- and oxaliplatin-GG adducts (the 3′-G or the 5′-G) and the pattern of misincorpo-

---

‡ Present address: Section on DNA Replication, Repair, and Mutagenesis, NICHD, National Institutes of Health, Bethesda, MD 20892-2725.

§ To whom correspondence should be addressed. Tel.: 919-966-3286; Fax: 919-966-2852; E-mail: Stephen_Chaney@med.unc.edu.

[1] The abbreviations used are as follows: cisplatin, *cis*-diaminedichloroplatinum(II); oxaliplatin, (*trans-R,R*)-1,2-diaminocyclohexaneoxalatoplatinum(II); Pt(dach)Cl$_2$, (*trans-R,R*)-1,2-diaminocyclohexanedichloroplatinum(II); dach, (*trans-R,R*)-1,2-diaminocyclohexane; pol, polymerase; HIV-1 RT, human immunodeficiency virus 1 reverse transcriptase; HMG, high mobility group.

ration opposite the adduct (8–10). The conformation of the 6 nucleotide-gapped template bound to pol β has not been directly determined but is likely to be different from the conformation of primed single-stranded DNA bound to pol β (12). Studies on the efficiency, specificity (cisplatin *versus* oxaliplatin), and fidelity of translesion synthesis by pol β on primed single-stranded and 6 nucleotide-gapped templates also suggest that the manner in which the adduct binds to the active site of the DNA polymerase could have significant biological consequences. For example, pol β catalyzes 2.5-fold more translesion synthesis past oxaliplatin adducts than past cisplatin adducts in experiments using single-stranded DNA, but does not appear to differentiate between cisplatin and oxaliplatin adducts during 6 nucleotide gap filling DNA synthesis (9). In addition, the type of the DNA template used also influences the effect of platinum adducts on the nucleotide insertion fidelity of pol β (9).

In contrast to the situation with 6 nucleotide-gapped templates, the conformations of both primed single-stranded and single nucleotide-gapped templates bound to the active site of pol β are known and are quite different. For the primed single-stranded template, the double-stranded region is bound to the enzyme, whereas the single-stranded region does not interact with the polymerase and thus, has considerable flexibility (13). With a single nucleotide-gapped template both ends of the gap are bound to enzyme, resulting in a 90° bend in the template (12, 14). Steady-state and presteady-state kinetic analyses (15, 16) have shown that the catalytic efficiency and nucleotide insertion fidelity of pol β are strongly influenced by the type of DNA substrate (gapped *versus* non-gapped). Even though only the structure of primed single-stranded template is likely to be relevant to translesion synthesis by pol β *in vivo*, usage of conformationally different DNA templates should serve as a good model system to study influence of template structure on translesion synthesis. Therefore, the present study was designed to evaluate how the use of single nucleotide-gapped DNA templates would affect the efficiency, carrier ligand specificity, and nucleotide insertion fidelity of DNA synthesis past Pt-DNA adducts by pol β.

EXPERIMENTAL PROCEDURES

Construction of Platinum Adduct-containing Templates—Primer-templates were constructed from synthetic oligonucleotides as described previously (8). Briefly, platination reactions were carried out with aquated derivatives of cisplatin (Sigma) and the active biotransformation product of oxaliplatin, Pt(dach)Cl$_2$ (provided by Dr. S. D. Wyrick, UNC). Platination of a 12-mer oligonucleotide containing a single GG sequence within a *Stu*I restriction site (TCTA<u>GG</u>CCTTCT) was performed for 2 h at 37 °C in the dark with a 2:1 drug/oligonucleotide ratio. The oligonucleotides containing single platinum adducts were separated from unplatinated oligonucleotides by 20% polyacrylamide gel electrophoresis.

The templates used for primer extension and steady-state kinetic experiments are listed in Fig. 1. DNA templates (44-mer), with or without platinum adduct, were constructed as described previously (8). Briefly, platinated 12-mer or undamaged 12-mer (used for assembling control DNA templates) were ligated with the 14-mer on the 5′-end and an 18-mer on the 3′-end of the template using a 35-mer scaffold. After 16 h of ligation at 16 °C by T4 DNA ligase, templates were restricted by *Stu*I to ensure the absence of any unplatinated oligonucleotides and purified on 12% denaturing polyacrylamide gels. Control experiments were performed to ensure the purity of platinated templates as described previously (8).

The 24- or 25-mer primers were ^{32}P 5′-end-labeled. The downstream oligonucleotides (19- and 18-mer) used to form single nucleotide-gapped templates were 5′-end phosphorylated with unlabeled ATP. DNA substrates were prepared by annealing undamaged or platinated 44-mer templates with primers and downstream oligonucleotides at a 1.2:1:2 molar ratio. Annealing efficiencies were >99%, as evidenced by the different mobility of the ^{32}P-labeled primers before and after hybridiza-

tion to the template on non-denaturing polyacrylamide gels (data not shown).

Steady-State Polymerization Kinetics—Recombinant human pol β was generously provided by Dr. S. Wilson (NIEHS, National Institutes of Health). The steady-state kinetic parameters K_m and V_{max} for dCTP incorporation were measured as a function of deoxynucleotide concentration (17, 18). Single nucleotide-gapped DNA templates (150 fmol) were incubated at 37 °C in 10 μl-reaction mixtures containing 50 mM Tris-HCl, pH 8.0, 10 mM MgCl$_2$, 2 mM dithiothreitol, 20 mM NaCl, 200 μg/ml bovine serum albumin, 2.5% glycerol, 5 fmol of pol β, and variable concentrations of dCTP. To determine the efficiency of nucleotide incorporation opposite the 3′-G, dCTP concentrations ranged from 1 to 8 μM for the undamaged template and from 16 to 256 μM for the platinated templates. To determine efficiency of nucleotide incorporation opposite the 5′-G, dCTP concentrations ranged from 0.03 to 0.5 μM for the undamaged template, from 16 to 256 μM for the cisplatin-containing templates and from 0.25 to 4 μM for the oxaliplatin-containing template. Reactions were terminated by mixing with 0.7 volumes of formamide-loading dye containing 500 mM EDTA, 0.1% bromphenol blue in 90% formamide and were then immediately transferred onto ice for 5 min. Products were resolved by denaturing polyacrylamide gel electrophoresis (8 M urea, 16% acrylamide, 4 h at 2000 V) and then visualized and quantified using a Molecular Dynamics PhosphorImager and Image-Quant software. Initial time-course studies indicated that under standard conditions product formation was linear (*i.e.* conforms to steady-state kinetics) for up to 4 min. Therefore, reactions were performed for 1 min for control DNA templates and for 2 min for platinated DNA templates. Less than 20% of the primers were extended under these conditions. The velocity of dCTP incorporation opposite the template 3′-G and 5′-G sites was determined as described previously (17, 18). V_{max} (the maximum reaction velocity) and K_m (dCTP concentration at which the reaction velocity is half-maximal) were determined from a Hanes-Woolf plot by linear least squares fit (18). Values for the apparent k_{cat} were calculated based on the assumption that pol β was fully active. The efficiency of nucleotide insertion by pol β was calculated as k_{cat}/K_m. To facilitate comparison of values for different platinum adducts, the relative insertion efficiency f_{rel} was calculated as $f_{rel} = (k_{cat}/K_m$ for Pt)/(k_{cat}/K_m for control). Because the steady-state kinetic analysis utilized in these experiments produces an apparent rather than a true V_{max} (17, 18), V_{max} and k_{cat} values in the literature are reported in a variety of units. The k_{cat} values we report were obtained by dividing V_{max} (in nM primer extended per min) by the enzyme concentration (0.5 nM). To compare these data with the V_{max} and V_{max}/K_m values reported in our previous kinetic analysis of translesion synthesis by pol β with different DNA templates (9), these k_{cat} and k_{cat}/K_m values must be divided by 30. To compare these data with V_{max} values reported as nM min^{-1}, these k_{cat} values must be multiplied by 5.

Primer Extension Assays Using Individual Nucleotides—To compare the pattern of misincorporation opposite Pt-GG adducts on primed single-stranded and gapped DNA templates, primer extension assays were performed using each dNTP individually as described previously (9). DNA templates (200 fmol expressed as primer termini) were incubated with 5 fmol of pol β at 37 °C for 30 min in 10-μl reactions containing 5 mM of each dNTP individually.

Kinetic Misincorporation Assays—To measure nucleotide misinsertion opposite Pt-GG adducts, 150 fmol of single nucleotide-gapped DNA substrates were incubated with 5 fmol of pol β and variable concentrations of dTTP or dATP. Reactions were performed for 5 min for undamaged DNA templates and 10 min for platinated DNA templates. dTTP concentrations ranged from 5 to 100 μM for undamaged and from 250 to 5000 μM for platinated templates. dATP concentrations ranged from 25 to 400 μM for undamaged and from 200 to 3600 μM for platinated templates. The kinetics of nucleotide misincorporation opposite platinated and undamaged GG sites were determined as described above. The misinsertion frequency (f_{mis}) was determined as the ratio of insertion efficiencies (k_{cat}/K_m) for incorrect and correct nucleotides. The relative misinsertion frequency was determined as $f_{mis.rel} = (f_{mis-Pt})/(f_{mis-control})$.

RESULTS AND DISCUSSION

In a previous study (9) we performed a kinetic analysis of nucleotide incorporation opposite Pt-GG adducts in a 5′-AGGC-3′ sequence by pol β using primed single-stranded DNA templates and 6 or 5 nucleotide-gapped DNA templates. In those studies, cisplatin-GG adducts inhibited nucleotide incorporation to a greater extent than oxaliplatin-GG adducts when primed single-stranded templates were used, but pol β did not
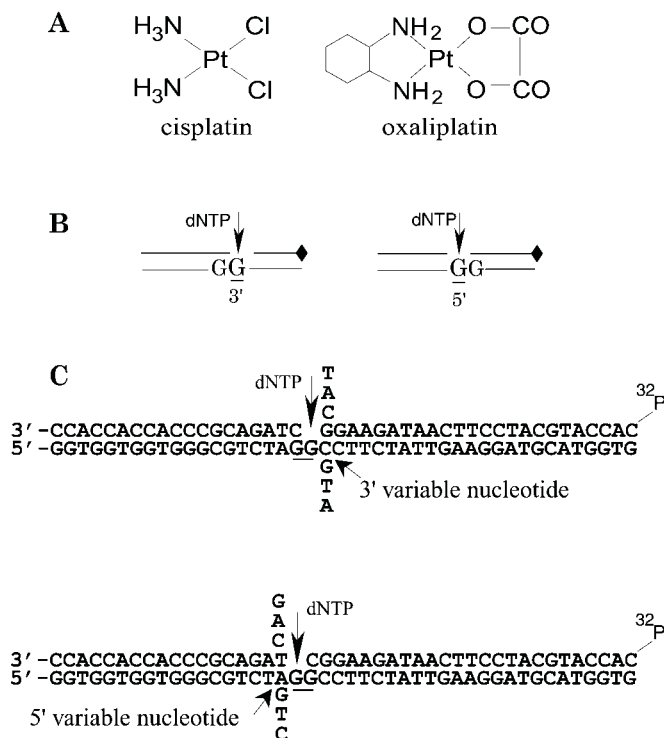
A

cisplatin   oxaliplatin

B

C

FIG. 1. **Chemical structure of the platinum complexes (*A*), configuration (*B*), and sequence (*C*) of single nucleotide-gapped DNA templates used in primer-extension and kinetic studies.** The site-specifically modified DNA templates were constructed using a combination of synthetic oligonucleotides as described under "Experimental Procedures." *B* shows a schematic representation of the DNA template used to determine nucleotide incorporation opposite the 3'- and 5'-G. The *top panel* of *C* shows the sequences of the template, upstream primer, and downstream acceptor used to measure nucleotide incorporation opposite the 3'-G. It also shows the variations in the sequence of the template and primer that were used to assess the effect of changes in the base 3' to the target site on the efficiency of correct nucleotide incorporation and the pattern of misinsertion. The *bottom panel* of *C* shows the sequences of the template, upstream primer, and downstream acceptor used to measure nucleotide incorporation opposite the 5'-G, along with the changes in sequence of the template and acceptor used to assess the effect of the base 5' to the target base. The GG sites of platinum adduct binding are *underlined*. In addition to the templates shown here, primed single-stranded templates (in which downstream oligonucleotides were omitted) and templates with 5 or 6 nucleotide gaps (in which downstream oligonucleotide was a 14-mer) were used to compare pattern of misincorporation on structurally different DNA templates. These templates have been described previously (9).

discriminate between cisplatin and oxaliplatin adducts during short gap filling. In the present study we have examined the catalytic efficiency and fidelity of pol β on DNA templates with a single nucleotide gap opposite the 3'- or 5'-G of the 5'-AGGC-3' sequence in both undamaged templates and templates containing a single cisplatin- or oxaliplatin-GG adduct (Fig. 1). These experiments are of interest because the conformation of this type of DNA template bound to pol β is very different from the templates with platinum adducts that have been analyzed previously (14).

Effect of DNA Template Structure on Efficiency of dCTP Incorporation—We performed steady-state kinetic assays for dCTP insertion opposite the template 3'- and 5'-G on undamaged templates and templates with cisplatin and oxaliplatin adducts by measuring nucleotide insertion at the first template site adjacent to the primer terminus (18). All experiments were carried out in the presence of a 30-fold excess of template over enzyme. The results are summarized in Table I. One striking observation was the 10-fold lower dCTP incorporation efficiency (k_{cat}/K_m) opposite the 3'-G relative to the 5'-G on un-

damaged single nucleotide-gapped DNA. This appears to be primarily an effect of sequence context on dCTP incorporation efficiency (see below). However, the influence of sequence context on the efficiency of dCTP incorporation opposite the guanines also depends on template structure, because no significant differences were observed in the k_{cat}/K_m for dCTP incorporation opposite the 3'- and 5'-G in the same sequence context with longer gapped or primed single-stranded DNA templates (9).

The enzyme concentration, template concentration, and template sequence used in these experiments are identical to those used in our previous study of pol β (9). Thus, the kinetic parameters obtained in this study can be directly compared with the kinetic parameters reported in our previous study (9). This allows a comparison of the efficiency and fidelity of translesion synthesis past platinum-DNA adducts by pol β with single nucleotide-gapped templates (this study), 5 or 6 nucleotide-gapped templates (9), and primed single-stranded templates (9). Such a comparison indicates that the use of single nucleotide-gapped DNA results in an increase in the efficiency of nucleotide insertion (k_{cat}/K_m) by pol β on undamaged templates. Thus, dCTP incorporation opposite the 3'- and 5'-G was 2.5–30 and 10–120 times more efficient on single nucleotide-gapped DNA than on the DNA with longer gaps and non-gapped substrates, respectively. This is similar to the results reported previously (15, 16).

Pt-GG adducts had different effects on the efficiency (k_{cat}/K_m) of dCTP insertion opposite the 3'-G and the 5'-G (Table I). There was a similar decrease in dCTP insertion efficiency across from the 3'-G of both platinum adducts (Table I). In contrast, the efficiencies of dCTP incorporation opposite the 5'-G were very different depending on carrier ligand of platinum adduct. There was a 170-fold decrease in insertion efficiency for dCTP incorporation opposite the 5'-G of cisplatin adduct. This is the most significant inhibition of pol β catalytic activity by a cisplatin adduct among all templates (gapped and non-gapped) tested (compare Table I and results in Vaisman and Chaney, Ref. 9). On the other hand, there was relatively little inhibition of pol β catalytic efficiency opposite the 5'-G of the oxaliplatin adduct (Table I and Ref. 9). Thus, our data show a very interesting variation in the carrier ligand specificity for dCTP incorporation as the DNA template changes from primed single-stranded to short-gapped (5 or 6 nucleotides) and to single nucleotide-gapped. With the primed single-stranded template, the efficiency of dCTP incorporation was about 2.5-fold greater for the oxaliplatin adduct opposite the 3'-G but was about the same for the two adducts opposite the 5'-G (9). With the short-gapped DNA (5 and 6 nucleotides), no significant differences were evident between templates with cisplatin and oxaliplatin adducts in the insertion efficiency of dCTP opposite either the 3'-G or the 5'-G (9). With the single nucleotide-gapped template the efficiency of dCTP incorporation was about 20-fold greater for the oxaliplatin adduct opposite the 5'-G but was about the same for both adducts opposite the 3'-G (this study).

These differences could be related to the differences in the conformation of the non-gapped and gapped DNA templates bound to pol β. The x-ray crystal structure of pol β with a non-gapped primed template shows that the double-stranded region of the template is aligned in the palm subdomain of the 31-kDa domain of polymerase (13, 19). The thumb region (C-terminal domain) closes around the DNA template to form a binding pocket for the incoming dNTP (13, 19). Whereas the double-stranded region and the template base for the incoming dNTP are tightly constrained by the thumb and fingers in this structure, the single-stranded region appears to have consid-

TABLE I

Steady-state kinetic analysis of dCTP insertion opposite Pt-GG adducts

Kinetic assays were performed using 5 fmol of pol β and 150 fmol of the primer-templates shown in Fig. 1*B*. Incubation time was 1 min for undamaged DNA substrates and 2 min for platinated DNA substrates. To determine the efficiency of nucleotide incorporation opposite the 3′-G, dCTP concentrations ranged from 1 to 8 μM for the undamaged template and from 16 to 256 μM for the platinated templates. To determine efficiency of nucleotide incorporation opposite the 5′-G, dCTP concentrations ranged from 0.03 to 0.5 μM for the undamaged template, from 16 to 256 μM for the cisplatin-containing templates and from 0.25 to 4 μM for the oxaliplatin-containing template. Kinetic parameters (K_m and k_{cat}) and insertion efficiency (k_{cat}/K_m) for dCTP incorporation by pol β were determined using Hanes-Woolf plots. The relative insertion efficiency was determined as $f_{rel} = (k_{cat}/K_{m/Pt})/(k_{cat}/K_{m/control})$. Data for k_{cat}, K_m, and k_{cat}/K_m are means ($\pm$ S.E.) from five to six different experiments using two independent template preparations.

Target (template)	Pt adduct	k_{cat}	K_m	k_{cat}/K_m	f_{rel}
		min^{-1}	μM		
3′-G	control	13.2 ± 1.5	5.8 ± 0.7	2.28 ± 0.12	
	cisplatin	1.4 ± 0.1	23.3 ± 3.6	0.060 ± 0.009	0.026
	oxaliplatin	2.6 ± 0.2	35.0 ± 3.6	0.074 ± 0.001	0.032
5′-G	control	4.5 ± 0.01	0.20 ± 0.04	23.4 ± 2.3	
	cisplatin	3.0 ± 0.02	27.7 ± 6.6	0.11 ± 0.02	0.005
	oxaliplatin	4.8 ± 0.03	1.5 ± 0.3	3.2 ± 0.3	0.14

erable flexibility (13, 19). In contrast, with single nucleotide-gapped DNA the amino-terminal 8-kDa domain of pol β binds to the downstream 5′-phosphate. This anchors both ends of the gap to the polymerase active site and results in a 90° bend in the template DNA (12). Although a crystal structure of pol β with a 6 nucleotide-gapped template is currently unavailable because of the difficulty in obtaining an appropriate crystal (12), it is likely that the conformation of the templates with longer gaps are different from the conformation of single nucleotide-gapped DNA. For example, with the one nucleotide-gapped DNA, the 5′-phosphate in the DNA gap is hydrogen bonded to Lys-68 (14), whereas for the DNA with a gap greater than one nucleotide, the 5′-phosphate is hydrogen bonded to Lys-35, Lys-68, Lys-72, and Lys-84 (20).

It is possible that the intrinsic conformation of the Pt-DNA adducts in primed single-stranded and single nucleotide-gapped DNA may also be different in solution. For example, dramatic conformational differences were observed in NMR solution structures of the (−)-*trans*-anti-[BP]dG adduct in single nucleotide-gapped and primed single-stranded DNA templates (21, 22). However, because of the severe constraints imposed on the gapped DNA when it binds to the active site of pol β, we feel that the greatest conformational differences between Pt-DNA adducts on the templates we have used are likely to be those imposed by the enzyme. These conformational differences probably play a critical role in determining the specificity, site and level of inhibition of nucleotide incorporation by the different Pt-DNA templates.

Nucleotide Misincorporation Opposite GGs on Undamaged and Platinated Templates—The conformation of the adduct at the active site of a DNA polymerase could also affect its mutagenicity and the spectrum of mutations that are produced. To obtain qualitative information about misincorporation across from the platinum adducts, extension studies by pol β were performed in the presence of 5 mM of either dCTP, dGTP, dTTP, or dATP. Fig. 2 shows the results of these experiments when both single-stranded and gapped templates were utilized. The presence of a platinum adduct did not influence the apparent pattern of nucleotide misincorporation. (Because the pattern of misincorporation was identical for templates with cisplatin and oxaliplatin adducts, only gels for templates with oxaliplatin adducts are shown). However, as could be predicted based on the different structures of pol β complexes with the non-gapped and gapped DNA templates, both the location (3′-G *versus* 5′-G) and spectrum (dNTP inserted) of misincorporation by pol β varied significantly depending on the structure of the DNA template (Fig. 2). dTTP misincorporation was detected for most DNA templates, except for incorporation opposite the 5′-G on

single-stranded templates. None of the other nucleotides were inserted opposite the 3′-G or 5′-G by pol β with primed single-stranded DNA templates and templates with 5 or 6 nucleotide gaps. However, the pattern of misincorporation opposite the template 3′-G and 5′-G with single nucleotide-gapped DNA templates was different. Pol β inserted dTTP much more readily than dATP opposite the 3′-G. Little or no misincorporation of dGTP opposite the 3′-G could be detected, even following a prolonged reaction time and at increased enzyme concentrations (data not shown). However, misincorporation of all three nucleotides was observed across from the 5′-G (Fig. 2).

To characterize the misincorporation efficiency on undamaged and platinated single nucleotide-gapped templates more quantitatively and to compare these data to previously reported kinetic parameters with non-gapped templates and templates with 5 or 6 nucleotide gaps (9), a steady-state kinetic analysis of dTTP and dATP incorporation was performed (Table II). Chagovetz *et al.* (16) have reported previously that the nucleotide insertion fidelity of pol β was 10–100 times higher on single nucleotide-gapped DNA compared with 6 nucleotide-gapped DNA and primer-template with no gaps. In contrast to this report, we observed an increased frequency (f_{mis}) of dTTP misincorporation opposite the undamaged 3′- and 5′-G residues for single nucleotide-gapped DNA compared with 5 or 6 nucleotide-gapped DNA and single-stranded DNA. The most likely explanation for the differences between our results and previous data (16) is the influence of the neighboring sequence context. The influence of sequence context on the fidelity of DNA polymerases has been reported previously (23, 24). For example, Mendelman *et al.* (24) reported that the misincorporation frequency for DNA polymerase α and AMV RT varied by 10-fold for the same mispair in different locations of the DNA template.

Cisplatin- and oxaliplatin-GG adducts had a similar effect on the efficiency (k_{cat}/K_m) of dTTP misincorporation with single nucleotide-gapped templates (Table II). Both adducts decreased the efficiency of dTTP incorporation by 30 to 40-fold opposite the 3′-G and 75 to 100-fold opposite the 5′-G. However, because cisplatin- and oxaliplatin-GG adducts had different effects on the efficiency of correct (dCTP) nucleotide incorporation (9), they also had very different effects on the frequency of misincorporation ($f_{mis} = (k_{cat}/K_m)_{dTTP}/(k_{cat}/K_m)_{dCTP}$; Table II). The frequency of dTTP misincorporation opposite the 3′-G was 1.6-fold less for oxaliplatin adducts than for cisplatin adducts. This was because of both a slight decrease in the efficiency of dTTP incorporation (Table II) and a slight increase in the efficiency of dCTP incorporation (Table I) for oxaliplatin adducts compared with cisplatin adducts. Opposite the 5′-G the
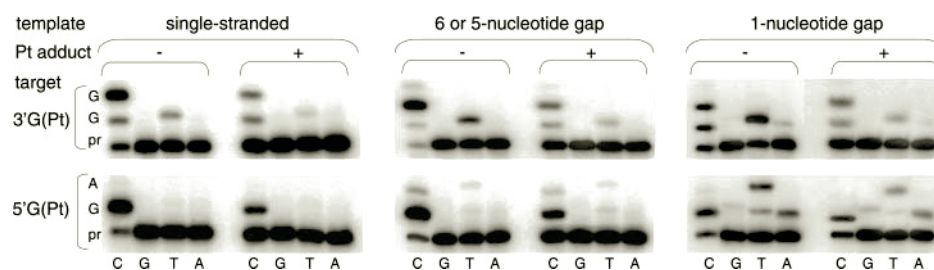
FIG. 2. **Specificity of nucleotide incorporation by pol β across from GG sites on undamaged DNA templates and templates with the oxaliplatin adduct.** Nucleotide incorporation studies were performed for 30 min using 200 fmol of DNA template, 5 fmol of pol β, and individual dNTPs present at a 5 mM concentration. (*C*, incubation with dCTP; *G*, incubation with dGTP; *T*, incubation with dTTP; and *A*, incubation with dATP.) Template sequence is indicated on the *left* (*pr*, primer).

<div align="center">

TABLE II

Steady-state kinetic analysis of dTTP and dATP insertion opposite Pt-GG adducts

</div>

Kinetic assays were performed using 5 fmol of pol β and 150 fmol of the single nucleotide-gapped DNA templates shown in Fig. 1*C*. Bands produced as a result of dATP misincorporation across from the 3′-G were detectable but were too weak for reliable measurement of kinetic parameters. Incubation time was 5 min for undamaged DNA templates and 10 min for platinated DNA templates. dTTP concentrations ranged from 5 to 100 μM for undamaged and from 250 to 5000 μM for platinated templates. dATP concentrations ranged from 25 to 400 μM for undamaged and from 200 to 3600 μM for platinated templates. Kinetic parameters (K_m and k_{cat}) and insertion efficiency (k_{cat}/K_m) for nucleotide insertion by pol β were determined using Hanes-Woolf plots. The misinsertion efficiency (f_{mis}) was determined as the ratio of incorrect (dTTP or dATP) to correct (dCTP) insertion efficiencies (k_{cat}/K_m for dCTP incorporation are from Table 1). The relative misinsertion frequency was determined as $f_{mis.rel} = (f_{mis/Pt})/(f_{mis/control})$. Data are means ($\pm$ S.E.) from five to seven different experiments using two independent template preparations.

Template base	dNTP	Pt adduct	k_{cat}	K_m	k_{cat}/K_m	f_{mis}	$f_{mis.rel}$
			min^{-1}	μM	$\times 10^3$	$\times 10^4$	
3′-G	dTTP	control	0.78 ± 0.15	29 ± 4	27.8 ± 0.6	118	
	dTTP	cisplatin	0.20 ± 0.02	240 ± 40	0.83 ± 0.18	138	1.17
	dTTP	oxaliplatin	0.28 ± 0.02	437 ± 62	0.64 ± 0.08	86	0.73
5′-G	dTTP	control	0.111 ± 0.006	4.6 ± 0.3	24 ± 2	10.6	
	dTTP	cisplatin	0.15 ± 0.02	634 ± 26	0.24 ± 0.02	21.8	2.06
	dTTP	oxaliplatin	0.19 ± 0.02	600 ± 55	0.32 ± 0.02	1.0	0.094
	dATP	control	0.165 ± 0.018	52 ± 10	3.2 ± 0.6	1.42	
	dATP	cisplatin	0.150 ± 0.019	702 ± 88	0.21 ± 0.02	19.1	13.4
	dATP	oxaliplatin	0.195 ± 0.012	742 ± 67	0.26 ± 0.02	0.81	0.57

frequency of dTTP misincorporation was 16-fold less for oxaliplatin adducts than for cisplatin adducts, primarily because of the relatively high efficiency of dCTP incorporation opposite the 5′-G of oxaliplatin adducts (Table I). This pattern of dTTP misincorporation was significantly different from that observed in the same sequence context with templates of different structure. The frequency of dTTP misincorporation opposite the 3′-G was 1.6 to 1.8-fold greater for oxaliplatin adducts than for cisplatin adducts with single-stranded and 6 nucleotide-gapped DNA templates (9). The pattern of dTTP misincorporation opposite the 5′-G could not be quantitatively compared with those templates because of the low frequency of dTTP misincorporation opposite the 5′-G with single-stranded and 5 nucleotide-gapped DNA templates.

In the qualitative experiments to determine the pattern of misincorporation with single nucleotide-gapped DNA, a significant misinsertion of dATP was observed opposite the 5′-G (Fig. 2). Therefore, we also determined kinetic parameters for dATP incorporation at this site (Table II). The qualitative assessment of misincorporation (Fig. 2) suggested that dTTP and dATP were misincorporated with similar efficiencies opposite the 5′-G on undamaged templates. However, quantitative measurements (Table II) showed that pol β favored misincorporation of dTTP by 6.5-fold compared with dATP on undamaged templates. This apparent discrepancy is explained by the fact that difference in the efficiency of dATP and dTTP incorporation was determined primarily by the differences in the K_m values. Because qualitative determination of the pattern of misincorporation was performed at saturating dNTP concentrations, the K_m-governed discrimination could not be detected in those experiments. This finding indicates the importance of quantitative analysis of primer extension on damaged and undam-

aged templates. In contrast to nucleotide incorporation on the undamaged template, pol β catalyzed dTTP and dATP misincorporation with similar efficiency on platinated templates (Table II). Thus, it is clear that both cisplatin- and oxaliplatin-GG adducts increase the frequency of dATP misincorporation relative to dTTP misincorporation. Finally, in comparing the oxaliplatin- and cisplatin-GG adducts, the frequency of dATP misincorporation opposite the 5′-G was 17-fold greater for the cisplatin adducts than for the oxaliplatin adducts.

The Effect of Sequence Context on the Efficiency and Fidelity of pol β—As described above, the efficiency of dCTP incorporation was 10-fold greater opposite the 5′-G than opposite the 3′-G of the 5′-AGGC-3′ sequence on an undamaged single nucleotide-gapped DNA template (Table I). In addition, the qualitative pattern of misincorporation on the single nucleotide-gapped template was dTTP~dATP≫dGTP for the 5′-G and dTTP≫dATP for the 3′-G (Fig. 2). With a primed single-stranded DNA template, dTTP misincorporation was seen opposite the 3′-G and no misincorporation could be observed opposite the 5′-G (Fig. 2). These data suggest that sequence context, as well as template structure, strongly influences both the efficiency and fidelity of pol β. To test this possibility, we systematically altered the bases 5′ and 3′ to the GG sequence with both single nucleotide-gapped and single-stranded templates. For the kinetic analysis of the dCTP incorporation, the measurements were made with the single nucleotide-gapped DNA template only (Fig. 1*C*), because no kinetic differences had been observed previously for the 3′- and 5′-G in primed single-stranded and longer gapped DNA templates (9). As can be seen in Table III, alteration of the base 5′ to the GG sequence had only a small effect on the efficiency of dCTP incorporation opposite the 5′-G. In contrast, the efficiency of dCTP

TABLE III

Influence of sequence context on the efficiency of dCTP insertion

Kinetic assays were performed for 1 min using 5 fmol of pol β and 150 fmol of the single nucleotide-gapped DNA templates shown in Fig. 1*C*. To determine the efficiency of nucleotide incorporation opposite the 3′-G, dCTP concentrations ranged from 1 to 8 μM for the template with C and T 3′ to the target site and from 0.03 to 0.5 μM for the template with G and A 3′ to the target site. To determine the efficiency of nucleotide incorporation opposite the 5′G, dCTP concentrations ranged from 0.03 to 0.5 μM. The insertion efficiency (k_{cat}/K_m) for dCTP incorporation by pol β were determined using Hanes-Woolf plots (see "Experimental Procedures"). Data are means ($\pm$ S.E.) from three different experiments.

Template base	Base 3′ to the target site	Base 5′ to the target site	k_{cat}/K_m
			$_M^{-1}\ min^{-1}$
3′-G	C	G	2.28 ± 0.12
	G	G	12.0 ± 2.1
	T	G	1.0 ± 0.2
	A	G	13.7 ± 2.4
5′-G	G	A	23.4 ± 2.3
	G	G	18.9 ± 2.5
	G	T	27.0 ± 2.8
	G	C	32.5 ± 3.1

incorporation was strongly influenced by the base 3′ to the adduct. The efficiency of dCTP incorporation opposite the 3′-G was low with a pyrimidine 3′ to the GG sequence. However, when a purine was 3′ to the GG sequence, the efficiency of dCTP incorporation opposite the 3′-G was increased significantly to a value that is similar to that seen opposite the 5′-G in the 5′-AGGC-3′ sequence. These data can best be explained by a model in which a purine 3′ to the templating G stabilizes it in the active site of pol β through stacking interactions. These data also suggest that the greater efficiency of dCTP incorporation opposite the 5′-G in the original 5′-AGGC-3′ sequence was primarily because of the presence of the adjacent 3′-G.

To test how local DNA sequence context influences nucleotide misinsertion, we carried out primer extension reactions with individual nucleotides on templates with various nearest neighbors adjacent to the target site (Fig. 3). On single nucleotide-gapped DNA, with a purine 3′ to the target site, dTTP misincorporation was about 2 times higher than dATP misincorporation (Fig. 3*B*). With a pyrimidine 3′ to the target site, pol β inserted dTTP 50–85-fold more efficiently than dATP (Fig. 3*A*). In addition, the type of pyrimidine 3′ to the target site strongly influenced dNTP misincorporation. Levels of both dTTP and dATP misincorporation were 10–60-fold higher with C 3′ to the target site than with T 3′ to the target site. In contrast, the template base 5′ to the target site did not produce a significant impact on the relative levels of dTTP and dATP misincorporation. On primed single-stranded DNA templates, dTTP misincorporation could be detected only when C was 3′ to the target site (Fig. 3, *C* and *D*). These data need to be interpreted with caution, because they have not been confirmed by detailed kinetic analysis of misincorporation in different sequence contexts. However, the data do suggest that the previously observed differences in the pattern of misincorporation opposite the 3′- and 5′-G in the 5′-AGGC-3′ sequence are largely because of effects of the sequence context on the specificity of misincorporation. These data are also in agreement with previous studies that showed that the base 3′ to the target site has a significant effect on the misincorporation efficiency by pol β (23, 24). We have not examined the effect of sequence context on the efficiency and fidelity of translesion synthesis past cisplatin- and oxaliplatin-GG adducts because of the need to locate the platinum adduct in a restriction site for purposes of purification of the platinated 44-mer and because of the difficulty obtaining a unique platinum adduct in a GG sequence
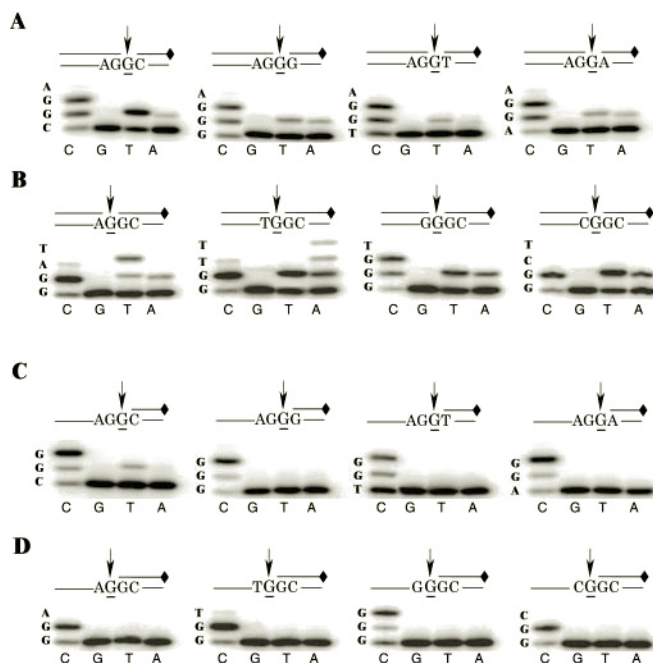

FIG. 3. **Nearest neighbor influence on the specificity of nucleotide incorporation by pol β opposite the 3′-G (*A* and *C*) and the 5′-G (*B* and *D*) on single nucleotide-gapped (*A* and *B*) and single-stranded (*C* and *D*) DNA templates.** Nucleotide incorporation studies were performed for 30 min using 200 fmol of DNA template, 5 fmol of pol β, and individual dNTPs present at a 5 mM concentration. (*C*, incubation with dCTP; *G*, incubation with dGTP; *T*, incubation with dTTP; and *A*, incubation with dATP.) Template sequence is indicated on the *left*, template structure and position of the target site (*underlined*) is shown on the *top*. ♦ represents the ^{32}P-labeled primer.

with G either 3′ or 5′ to the adduct. However, the sequence context of Pt-GG adducts is known to affect their mutagenicity (25, 26) and Pilch *et al.* (27) have recently shown that sequence context affects the conformation of Pt-GG adducts. Thus, it is likely that sequence context will also affect both the efficiency and fidelity of translesion synthesis past Pt-GG adducts by pol β and other DNA polymerases.

Summary—In our previous reports (9) we have shown that eukaryotic DNA polymerases pol β, γ, ζ, and η all bypass oxaliplatin-GG adducts to a greater extent than cisplatin-GG adducts. However, the efficiency and accuracy of this bypass was different for the each polymerase. This suggested that translesion replication past Pt-DNA adducts was determined by both the structure of the adduct and the DNA polymerase involved in translesion synthesis. In the present study we show that the replication blocking potential and mutagenicity of Pt-DNA adduct is likely to be strongly influenced by constraints imposed on the template when it binds to the active site of the polymerase. In support of this hypothesis we have shown that for translesion synthesis past Pt-DNA adducts by pol β the specificity (cisplatin *versus* oxaliplatin), the site of discrimination (3′-G *versus* 5′-G), and the pattern of misincorporation is strongly dependent on the DNA template structure. These differences are most likely because of changes in the conformation of Pt-DNA adducts when structurally different DNA templates are bound to the active site of pol β. Thus, whereas the conformation of DNA adducts is most often studied in solution in the absence of any protein, these data suggest that conformational studies of DNA adducts in the active site of the polymerases responsible for translesion synthesis will be important for an understanding of mutagenesis mechanisms. Our data also show that sequence context affects the efficiency of correct nucleotide incorporation and the pattern of misincorporation by pol β. Whereas these data were obtained with

undamaged DNA, sequence context is also likely to affect the efficiency and fidelity of translesion synthesis past Pt-DNA adducts as well. Elucidation of structural features of Pt-DNA adducts in the active site of pol β will be required to define the mechanism of these effects.

REFERENCES

1. Eastman, A. (1987) *Pharmacol. Ther.* **34,** 155–166
2. Woynarowski, J. M., Chapman, W. G., Napier, C., Herzig, M. C. S., and Juniewicz, P. (1998) *Mol. Pharmacol.* **54,** 770–777
3. Gelasco, A., and Lippard, S. J. (1998) *Biochemistry* **37,** 9230–9239
4. Herman, F., Kozelka, J., Stoven, V., Guittet, E., Girault, J. P., Huynh-Dinh, T., Igolen, J., Lallemand, J. Y., and Chottard, J. C. (1990) *Eur. J. Biochem.* **194,** 119–133
5. Takahara, P. M., Rosenzweig, A. C., Frederick, C. A., and Lippard, S. J. (1995) *Nature* **377,** 649–652
6. Yang, D., van Bloom, S. S. G. E., Reedijk, J., van Bloom, J. H., and Wang, A. H. J. (1995) *Biochemistry* **34,** 12912–12920
7. Fink, D., Nebel, S., Aebi, S., Zheng, H., Cenni, B., Nehme, A., Christen, R. D., and Howell, S. B. (1996) *Cancer Res.* **56,** 4881–4886
8. Vaisman, A., Lim, S. E., Patrick, S. M., Copeland, W. C., Hinkle, D. C., Turchi, J. J., and Chaney, S. G. (1999) *Biochemistry* **38,** 11026–11039
9. Vaisman, A., and Chaney, S. G. (2000) *J. Biol. Chem.* **275,** 13017–13025
10. Vaisman, A., Masutani, C., Hanaoka, F., and Chaney, S. G. (2000) *Biochemistry* **39,** 4575–4580
11. Kunkel, T. A., and Wilson, S. H. (1998) *Nat. Struct. Biology.* **5,** 95–99
12. Pelletier, H., Sawaya, M. R., Wolfle, W., Wilson, S. H., and Kraut, J. (1996) *Biochemistry* **35,** 12742–12761
13. Pelletier, H., Sawaya, M. R., Kumar, A., Wilson, S. H., and Kraut, J. (1994) *Science* **264,** 1891–1903
14. Sawaya, M. R., Prasad, R., Wilson, S. H., Kraut, J., and Pelletier, H. (1997) *Biochemistry* **36,** 11205–11215
15. Ahn, J., Kraynov, V. S., Zhong, X., Werneburg, B. G., and Tsai, M. D. (1998) *Biochem. J.* **331,** 79–87
16. Chagovetz, A. M., Sweasy, J. B., and Preston, B. P. (1997) *J. Biol. Chem.* **272,** 27501–27504
17. Boosalis, M. S., Petruska, J., and Goodman, M. F. (1987) *J. Biol. Chem.* **262,** 14689–14696
18. Creighton, S., Bloom, L. B., and Goodman, M. F. (1995) *Methods Enzymol.* **262,** 232–256
19. Beard, W. A., and Wilson, S. H. (1998) *Chem. Biol.* **5,** R7-R13
20. Beard, W. A., and Wilson, S. H. (2000) *Mutat. Res.* **460,** 231–244
21. Cosman, M., Hingerty, B. E., Geacintov, N. E., Broyde, S., and Pate, D. J. (1995) *Biochemistry* **34,** 15334–15350
22. Feng, B., Gorin, A., Kolbanovskiy, A., Hingerty, B. E., Geacintov, N. E., Broyde, S., and Patel, D. J. (1997) *Biochemistry* **36,** 13780–13790
23. Efrati, E., Tocco, G., Eritja, R., Wilson, S. H., and Goodman, M. F. (1997) *J. Biol. Chem.* **272,** 2559–2569
24. Mendelman, L. V., Boosalis, M. S., Petruska, J., and Goodman, M. F. (1989) *J. Biol. Chem.* **264,** 14415–14423
25. Bubley, G. J., Ashburner, B. P., and Teicher, B. A. (1991) *Mol. Carcin.* **4,** 397–406
26. de Boer, J. G., and Glickman, B. W. (1989) *Carcinogenesis* **10,** 1363–1367
27. Pilch, D. S., Dunham, S. U., Jamieson, E. R., Lippard, S. J., and Breslauer, K. J. (2000) *J. Mol. Biol.* **296,** 803–812